

THE NUMERICAL STUDY OF THE HYDRAULIC DAMPENER EFFICIENCY FOR MINIMIZATION OF THE FLOATING OIL PLATFORM PITCHING UNDER THE ACTION OF THE SEA ROUGHNESS

Sergey Lupuleac

Saint Petersburg Polytechnical University, Russia

Alexander Bol'shev

Saint Petersburg Polytechnical University, Russia

Julia Shinder

Saint Petersburg Polytechnical University, Russia

Alexander Ulanov

Saint Petersburg Polytechnical University, Russia

Eugene Toropov

Central Design Bureau for Marine Engineering "Rubin", St Petersburg, Russia

Andrey Gintovt

Central Design Bureau for Marine Engineering "Rubin", St Petersburg, Russia

ABSTRACT

The relatively simple and effective mathematical model taking into account the influence of the hydraulic dampeners onto the dynamic behavior of the floating oil platforms is presented in this work.

The CFD (Computational Fluid Dynamics) approaches are used herein for determination of the dynamic drag coefficients of different dampeners performing sinusoidal vibrations in the viscous fluid. The numerical algorithm includes the simulation of the flow over moving dampener, the calculation of the loads from the moving water onto the dampener and the determination of the dynamic drag coefficients and attached masses. These parameters are used in the mathematical model simulating the behavior of the anchored platform under the action of the sea roughness.

1. INTRODUCTION

The state-of-art CFD codes (such as Ansys Fluent, Ansys CFX, Adapco Star CD etc.) allow performing simulation of the floating object movement under the loads from the flowing water. However this kind of simulations requires sufficiently large amount of resources (e.g. powerful multiprocessor computers). On the other hand there is a number of codes that simulate the dynamic behavior of the floating objects taking into account the forces from the moving water obtained by the ideal liquid model. These codes allow obtaining the results without use of the excessive

resources but do not take into account properly the viscous effects that in some cases can be significant (see Younis et al., 2001).

The presented work was devoted to the development and implementation of the combined computational technique that uses the results of relatively simple CFD simulations and the ideal liquid model for modeling the anchored oil platform behavior.

2. MATHEMATICAL MODEL

The object of research is the floating oil platform with hydraulic dampeners (see Fig. 1). The objective is to evaluate the efficiency of different dampener designs for minimization of the platform pitching under the action of the sea roughness.

The numerical algorithm used in presented work consists of the three stages:

Stage 1. The CFD simulation of the flow over test object making sinusoidal vibrations.

Stage 2. Decomposition of the hydrodynamic load onto several components by means of the Fourier-analysis.

Stage 3. The simulation of the dynamic behavior of the floating oil platform with consideration hydraulic dampener under the action of the sea roughness using the ideal liquid model with regard to parameters obtained in stage 2.

Now we will consider each stage in more details.

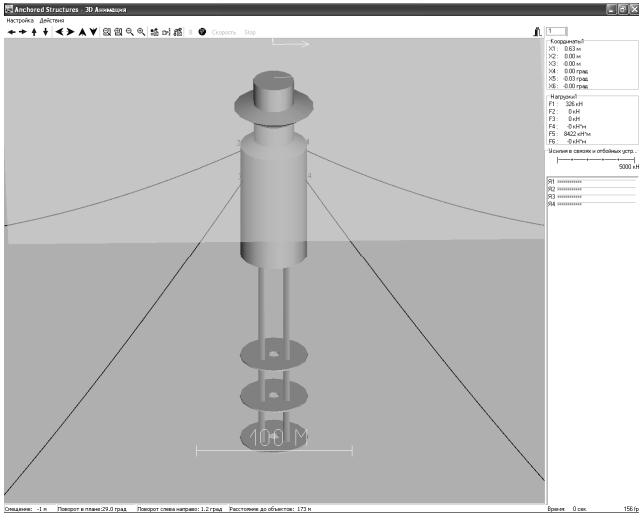


Figure 1: The floating oil platform with hydraulic damper (computer model in the Anchored Structures code)

2.1 Stage 1. CFD simulations

The possible test objects for these simulations are single hydraulic damper, system of hydraulic dampers or the whole floating oil platform equipped with dampeners. The 2D or 3D non stationary models are used depending of the test object design. The forced sinusoidal oscillations of the test object in the aquatic environment are simulated in the CFD codes Ansys Fluent and Ansys CFX. As a result of CFD analysis we obtain the hydrodynamic load acting on the test object as a function of time.

In this paper we present four different examples of test objects: the single circular disk dampener; the system of three circular disk dampeners; the perforated circular disk dampener; the whole floating oil platform.

The **single circular disk dampener** was considered mainly for validation purposes (Det Norske Veritas, 1991). We used 2D as well as 3D models. Figure 2 presents the results of 3D simulation in Ansys CFX of the flow over dampener.

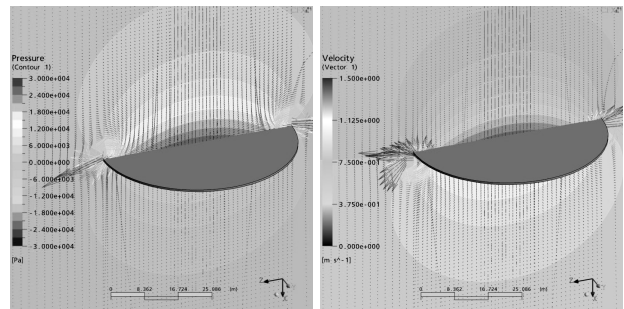


Figure 2: The flow over oscillating disk (the pressure and velocity fields in two positions)

The second example of test object for CFD simulations is the **system of three circular disk dampeners** (see Fig. 3, left). 2D model was applied in this case (see Fig. 3, right). The investigation of the damping capacity dependence from the distance between dampeners was of special interest here.

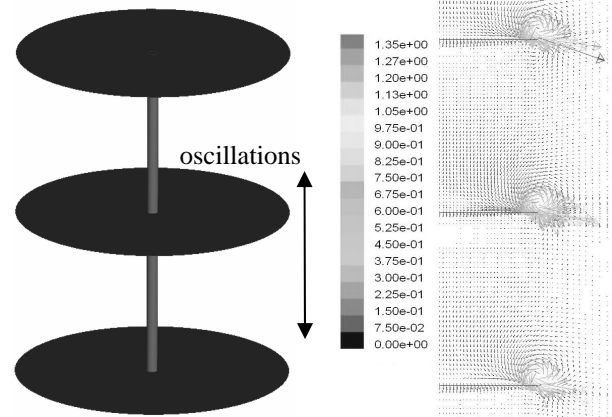


Figure 3: The system of three dampeners (left) and the flow over dampeners (velocity vectors)

The next example is the simulation of the flow over perforated dampeners (see Fig 4).

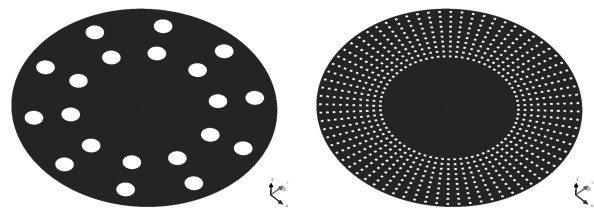


Figure 4: The examples of perforated dampeners

The 3D CFD model was implemented. Instead of the whole dampener we simulated only one sector. Computation domain, boundary conditions and CFD mesh are shown in Figure 5.

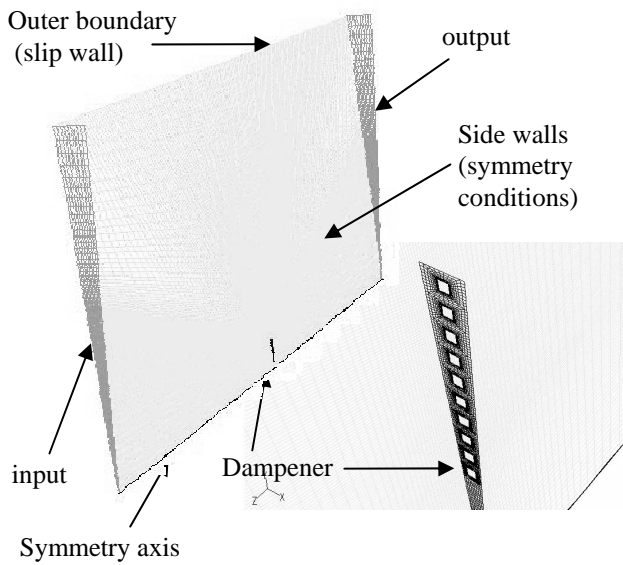


Figure 5: *Computation domain, boundary conditions and CFD mesh*

The computed instant field of velocity modulus in one case is presented in Figure 6

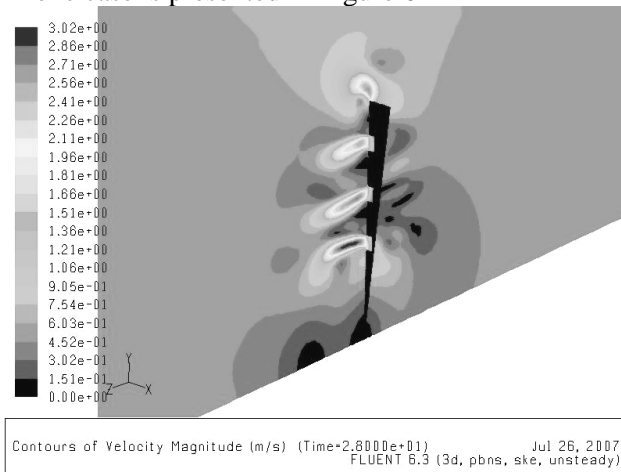


Figure 6: *Flow over perforated dampener. Instant field of velocity modulus.*

The last example of test object for CFD simulations is the floating oil platform presented in Figure 7. It is designed in such a way that some elements of its construction act like hydraulic dampeners.

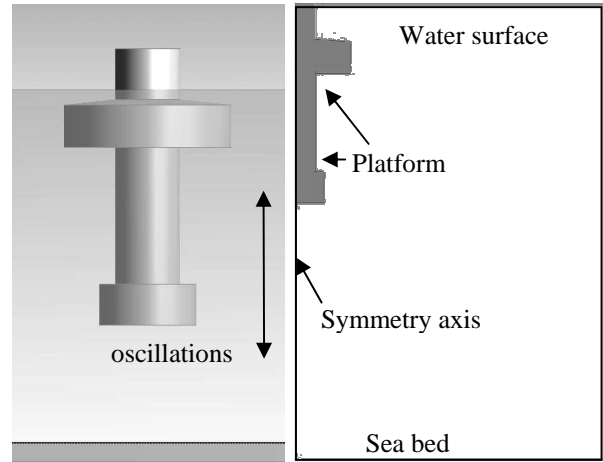


Figure 7: *Geometry model of the floating oil platform (left) and computation domain*

The 2D model was used for simulation of the flow over oscillating platform. Computation domain is shown in the right part of Figure 7.

Figure 8 shows the pressure distributions in four different time instances corresponding to different stages of the oscillation period.

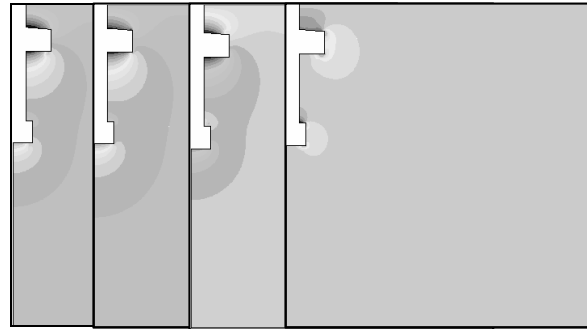


Figure 8: *Flow over oscillating platform. Pressure distribution in four instances.*

2.2 Stage 2. Hydrodynamic load decomposition

We assume that test object performs sinusoidal oscillations with amplitude A and period T . The vertical velocity v_y can be obtained from the following formula:

$$v_y(t) = \frac{2\pi A}{T} \sin\left(\frac{2\pi}{T}t\right) \quad (1)$$

The CFD simulations give us the dependence of hydrodynamic load F from time t . Figure 9 presents typical time distribution of the hydrodynamic load obtained from CFD. The vertical velocity of the test object is also shown in the same graph for convenience sake.

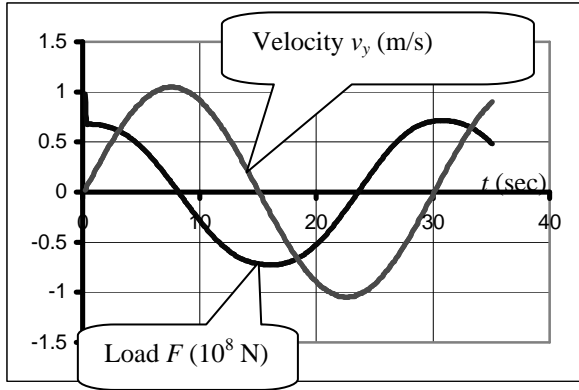


Figure 9: The time dependence of test object vertical velocity and hydrodynamic load

The hydrodynamic load F is split onto attached mass inertia force F_a , dynamic drag force F_v and the residual load F_r (see Fig. 10) as described below.

The component F_a is caused by the inertia of the attached mass of water. So it is proportional to the vertical component of test object acceleration that is obtained by differentiation of (1):

$$a_y(t) = A \left(\frac{2\pi}{T} \right)^2 \cos \left(\frac{2\pi}{T} t \right) \quad (2)$$

We choose the time value t_0 at the beginning of the stationary vibration phase, i. e. when the $F(t)$ function is already a periodical one.

We put

$$F_a(t) = C_{\cos} e_{\cos}(t), \quad (3)$$

where

$$e_{\cos}(t) = \sqrt{\frac{2}{T}} \cos \left(\frac{2\pi}{T} t \right)$$

and

$$C_{\cos} = \int_{t_0}^{t_0+T} F(t) e_{\cos}(t) dt.$$

Now we find attached mass of the water from the formula

$$m_a = \frac{F_a}{a_y}. \quad (4)$$

Next we determine the dynamic drag force F_v that is proportional to the square of velocity:

$$F_v(t) = C_{\sin} e_{\sin}(t) \quad (5)$$

where

$$e_{\sin}(t) = \text{sign} \left(\sin \left(\frac{2\pi}{T} t \right) \right) \sqrt{\frac{8}{3T}} \sin^2 \left(\frac{2\pi}{T} t \right)$$

(sign is signum function) and

$$C_{\sin} = \int_{t_0}^{t_0+T} F(t) e_{\sin}(t) dt.$$

The dynamic drag coefficient is obtained from the formula

$$C_v = \frac{2F_v(t)}{Sv_y^2(t)\rho}, \quad (6)$$

where S is the effective square of the test object and ρ is the water density.

And at last we define the residual load, subtracting F_v and F_a from F :

$$F'(t) = F(t) - F_a(t) - F_v(t). \quad (7)$$

Figure 10 gives the example of decomposition of hydrodynamic load. Usually the component F_v is much smaller than F_a , and it needs the accurate CFD analysis to compute it properly.

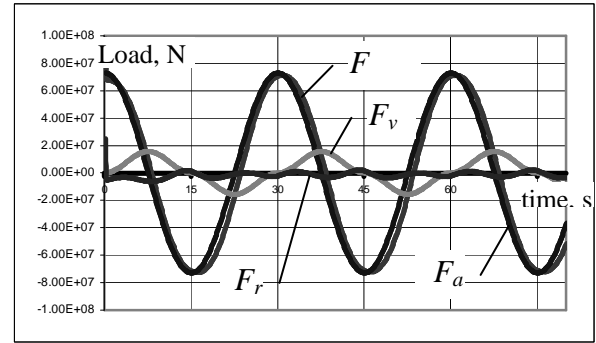


Figure 10: Decomposition of the hydrodynamic load

The values of attached mass m_a and dynamic drag coefficient C_v are used in subsequent analysis of floating platform dynamics (see item 2.3).

2.3 Stage 3. The simulation of whole marine structure dynamics with regard to parameters obtained in stage 2

As it was mentioned before, the dynamics of the whole analyzed marine structure is simulated in the Anchored Structures code (see Fig. 11) developed in Saint Petersburg Polytechnical University.

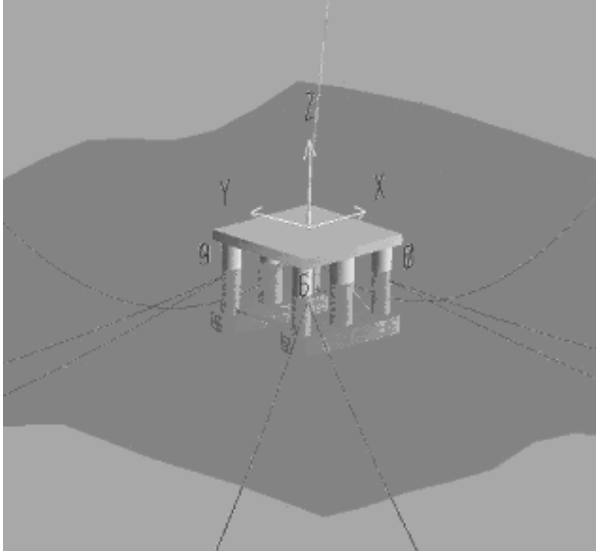


Figure 11: *The main window of the Anchored Structures code*

Let's consider the given anchored marine structure equipped with hydraulic dampeners that is exposed to the action of sea roughness, currents, wind, ice etc. The generalized displacement vector in six degrees of freedom \mathbf{X}_c (three displacements and three rotations) is governed by the following differential equation:

$$(\mathbf{M} + \mathbf{\Lambda})\ddot{\mathbf{X}}_c + \mathbf{B}\dot{\mathbf{X}}_c + \mathbf{C}_v\dot{\mathbf{X}}_c \left| \dot{\mathbf{X}}_c \right| - \mathbf{C}_R(\mathbf{X}_c) + \mathbf{R}(\mathbf{X}_c) = \mathbf{F}(t). \quad (8)$$

Here \mathbf{M} is extended mass and inertia moment matrix; $\mathbf{\Lambda}$ is the matrix of attached mass and inertia moments; \mathbf{C}_v is the drag coefficient matrix; \mathbf{C}_R is the restoring force vector; \mathbf{R} is the generalized vector of reactions (in anchors, moorings etc.) and \mathbf{F} is the vector of external forces (from waves, currents, wind etc.); $\dot{\mathbf{X}}_c$ and $\ddot{\mathbf{X}}_c$ are respectively the first and the second time derivatives of \mathbf{X}_c .

The parameters C_v and m_a obtained in stage 2 are used for determination of matrices \mathbf{C}_v and $\mathbf{\Lambda}$, respectively. All other parameters accountable in equation (8) are computed directly in the Anchored Structures code (in particular with use of ideal liquid model).

3. CONCLUSION

The described here approach was applied to simulation of the dynamics of floating platform equipped with hydraulic dampeners of various design (Lupuleac et al, 2006-2007). It was revealed

that perforated dampeners with relatively small porosity coefficient (like shown in Fig. 4) provide maximum damping effect. Also the systems of several dampeners (like one presented in Fig. 3) are also proved to be very effective.

4. ACKNOWLEDGEMENTS

This work was partially supported by Microsoft Corporation in the framework of Technical Computing Initiative (TCI) program.

Contributions by Mr Alexey Lipjainen in CFD model development are gratefully acknowledged.

5. REFERENCES

- Environmental conditions and environmental loads, 1991, Det Norske Veritas, *Classifications notes, No 30.5*
- Kareem A., 1983, Nonlinear dynamic analysis of compliant offshore platforms subjected to fluctuating wind, *Civil Engineering University of Houston, USA*
- Lupuleac, S., Shinder, J. et al. 2006-2007, Numerical simulation of the oscillation of disk dampener system submerging into water, *Research project Reports, St. Petersburg Polytechnical University*
- Pendyala, R., Jayanti, S., Balakrishnan, A.R., 2008, Flow and pressure drop fluctuations in a vertical tube subject to low frequency oscillations, In *Nuclear Engineering and Design, Volume 238, 178-187.*
- Petrauskas, C; Finnigan, T, 1994, Metocean criteria/loads for use in assessment of existing offshore platforms, In *Proceedings of 26th Annual Offshore Technology Con, Houston, Tx, Procs., Vol 3, 155-168.*
- Robert, A.G., 1977, Reduce of offshore platform dynamic response by tuned mass damper, USA.
- Younis, B. A., Teigen, P., and Przulj, V. P. , 2001, Estimating the hydrodynamic forces on a mini TLP with computational fluid dynamics and design-code techniques, In *Ocean Engineering, Volume 28, 585-602*